Appendix 1

SEASONALLY HYPERSALINE ESTUARIES IN MEDITERRANEAN-CLIMATE REGIONS

J. L. Largier *
Center for Coastal Studies, 0209
Scripps Institution of Oceanography
University of California, San Diego
La Jolla, CA 92093-0209

J. T. Hollibaugh
Tiburon Center
San Francisco State University
Tiburon, CA 94920

S. V. Smith
Department of Oceanography
University of Hawaii
Honolulu, HI 96822

Submitted to *Estuarine, Coastal and Shelf Science*

Abstract

Data collected in three Californian estuaries indicate that hypersaline conditions exist during the dry summers typical of a mediterranean climate. This observed accumulation of salt indicates surprisingly long residence times in small basins which have free exchange with the ocean. The semi-isolation of the inner basin leads to a large build-up or severe depletion of nutrients, pollutants and plankton in these systems. Of concern are the trends to increase pollutant loading in the same systems that are experiencing an increase in residence times owing to freshwater extraction in the watershed. In these mediterranean climate basins, small changes in climate or watershed management can lead to large changes in the biogeochemistry and ecology of the system.

Keywords

hypersalinity

inverse estuary

residence time

longitudinal diffusivity

DIP concentration

seasonal cycle

mediterranean climate

Introduction

We have collected several years of hydrographic data from Tomales Bay near San Francisco and some comparative data from San Diego and Mission Bays in San Diego (Fig. 1). Water temperature and salinity exhibit a recurrent seasonal cycle and a common longitudinal structure in these estuaries. During the long, dry, mediterranean-climate summer, evaporative loss of freshwater exceeds the supply of freshwater via precipitation and runoff. The basin water becomes saltier to the extent that the basin salinity significantly exceeds that in the ocean (i.e., hypersalinity, see note 1). A prerequisite for hypersalinity is the long residence of water in this evaporative basin. While the most extreme seasonal hypersalinity and precipitation of salt occurs in those estuaries that close at the mouth during summer (eg., Milnerton Lagoon, South Africa, Day, 1981, pp. 315-316), we focus on the more general case of estuaries that maintain a permanent connection with the ocean.

The occurrence of hypersalinity, although primarily a symptom of long residence in the inner basin, bears some relation to the dynamics of exchange between the basin and the ocean. The density of water is a function of salinity and temperature (Gill, 1982, Appendix 3), so that if the basin water is sufficiently hypersaline and/or cold, it will be denser than the ocean water and it will tend to drain out of the basin, being replaced by less dense ocean water. This is referred to as an inversely (see note 1) stratified estuary (Pritchard, 1967). Alternatively, if the basin water is less saline and/or warmer than the ocean water, it will tend to spread seaward over the inflowing dense ocean water. This is a classically stratified estuary (Pritchard, 1967). As is shown below, the occurrence of summer hypersalinity in mediterranean estuaries is commonly associated with warm water and weak density gradients which are insufficient to lead to significant vertical exchange flows.

There are previous studies of large evaporative seas, such as the Mediterranean Sea (Lacombe and Richez, 1982), the Red Sea (Phillips, 1966), the Gulf of California (Bray and

Robles, 1991) and Spencer Gulf (Nunes Vaz, et al, 1990), and some limited discussion of tropical estuaries such as Laguna Madre (Smith, 1988), Fleuve Cassamance (Pages and Debenay, 1987) and small northern Australian estuaries (Wolanski, 1986). However, there is an absence of previous work recognizing the widespread occurrence of seasonal hypersalinity in numerous mid-latitude, west-coast estuaries. While dynamical analyses are lacking, there are enough reports of hypersalinity in a variety of these systems (Table 1) that one may argue that this is a major estuarine class, characteristic of mediterranean climates. The alternating between classical estuary (net dilutive basin) during the wet winter and hypersaline estuary (net evaporative basin) during the dry summer is a response to the seasonal climate, in a hydrological system with appropriate watershed and estuarine characteristics. Changes in climate, due to global cycles and trends, and changes in the inflow hydrograph, due to watershed management, may lead to large changes in the hydrodynamic residence time, biogeochemistry and ecology of the system. At the equatorward extreme of these regions, the net evaporative season may last for several years, resulting in persistent and intense hypersaline conditions (as in Baja California, Mexico), whereas at the poleward extreme of these regions the net dilution season tends to persist, resulting in the absence of hypersaline conditions throughout the year (as in northern California).

Observed Seasonal Structure

In winter, mediterranean estuaries are usually classical in nature - there is substantial freshwater inflow and the system is stratified (Fig. 2). For some time after the winter rains stop, drainage of the watershed ensures a net inflow of freshwater and salinities remain below the oceanic ambient, although temperatures increase markedly. By mid-summer the temperature has attained a steady state whereas salinity continues to increase (Figs. 2 and 3). The salinity maximum in late summer is thus matched by a temperature maximum and, typically, the density of basin water is less than that of ocean water. Maximum density and inverse conditions occur as estuarine temperatures decrease due to surface cooling in autumn. Hypersalinity may weaken as

the balance between ocean-bay exchange and evaporative loss adjusts to weaker net evaporation in autumn, but it is only in response to winter rain and increased freshwater runoff that basin that basin salinities drop below that in the ocean (Fig. 2).

The seasonal fluctuations in salinity can be described by a time-varying salt balance. Expecting dispersion and residence time to vary as a function of distance from the head of the estuary, and assuming that all runoff enters at the landward end of the basin, a one-dimensional salt balance is approximated by:

$$\partial_t S = \partial_x [K_x \partial_x S - (Q_f/WH + Px/H - Ex/H)S] \qquad (1)$$

where $S(x,t)$ is salinity, $E(t)$ is evaporation rate, $P(t)$ is precipitation rate, $Q_f(t)$ is stream inflow, $H(x)$ is water depth, $W(x)$ is width of basin, t is time, x is longitudinal distance from the head and $K_x(x,t)$ is longitudinal diffusivity. In summer, the net freshwater budget is negative $Q_f/Wx + P - E < 0$ so that there is a net inflow of ocean water and the advective salt flux is into the basin. For the salt content of this evaporative basin (or any net evaporative part of it) to be constant, the diffusive salt flux must be seaward, which requires $\partial_x S < 0$, ie., increasing salinity with distance from the mouth (Fig. 3). Towards the head, however, freshwater inflow becomes more important (if non-zero). For parts of the bay described by $x < x_c$, where $x_c = Q_f/(E-P)W$, the net freshwater budget is positive and a constant salt content in this net dilutive part requires $\partial_x S > 0$, ie., decreasing salinity towards the head. In essence, the seasonal cycle in salinity $S(x,t)$ is driven by the seasonal cycles in evaporation, precipitation and runoff, with some interactive feedback through $K_x(t)$. The salinity decrease from the summer maximum to the winter minimum is primarily a result of increased freshwater inflow Q_f. The salinity increase from winter to summer is initially due to large K_x, while the basin-ocean density difference is large (stratified exchange), and then due to net evaporation. If the summer K_x/x is large relative to evaporative losses, a steady state $\partial_t S=0$ is attained rapidly but with weak hypersalinity (small

$\partial_x S$), whereas if K_x/x is small, a steady state will only occur later, but with a stronger hypersaline signal (large $\partial_x S$). In Mission Bay, P and Q_f go to zero during spring and remain zero during summer and autumn. A 2 ppt hypersalinity is built over 2 months, then persists as a quasi-steady state for about 5 months from late June until late November 1992 (Fig.2). During September-October, the strength of the hypersalinity weakens slowly as the days shorten and the net daily evaporation decreases.

During cooling in October-November, the density of the water in Mission Bay increases, eventually exceeding that in the ocean. Nevertheless, hypersalinity persists in the inner basin, indicating the absence of a flushing event associated with a dense outflow of cool hypersaline water. Any stratified exchange due to the 1 kg m^{-3} inverse longitudinal density gradient appears to be tidally transient and it results in a negligible increase in diffusivity K_x over that due to tidal dispersion mechanisms. It is expected that the vertical mixing resulting from bottom tidal stresses precludes stratification during much of the tidal cycle (Linden and Simpson, 1988; Nunes Vaz, et al, 1989). Relative to the deeper evaporative seas (eg., Mediterranean and Red Seas), these shallow tidal basins require a large longitudinal density gradient for K_x to significantly exceed values observed in a homogeneous basin. Typically,hypersaline estuaries exhibit a vertically mixed structure, irrespective of whether the longitudinal density gradient is marginally inverse or marginally classical (Fig. 2), and the buoyancy-driven vertical circulation is negligible.

Observed Longitudinal Structure

Partially explained by the absence of buoyancy-driven vertical circulation, the weak estuary-ocean exchange required for the occurrence of hypersalinity also implies weak tidal exchange. Hypersalinity is observed in basins, or parts of basins, characterized by long,narrow, single-channel morphology (Table 1), where longitudinal tidal dispersion is weak. The dom-

inant and characteristic spatial structures in hypersaline systems are thus longitudinal, and we adopt a one-dimensional advection-diffusion approach.

A typical longitudinal structure is illustrated by the vertical CTD sections presented in Fig. 4. In the outer estuary, temperature increases markedly from the low values typical of the Californian coast while the increase in salinity is weak. Farther into the estuary, water is not exchanged as rapidly and significant salinity increases are observed, while temperature appears saturated. The density structure of the outer estuary is thus dominated by temperature, whereas the inner estuary is dominated by salinity structure. A density minimum may be observed in the inner estuary (eg., Fig. 4c). Some vertical stratification is observed in the regions of significant longitudinal density gradient, particularly in the deeper sections such as the outer part of San Diego Bay (Fig 4 and Chadwick, et al, 1994). However, this stratification is transient.

In all of the Californian estuaries that we have studied, there is negligible freshwater runoff in summer and salinities increase with distance from the ocean (as in Fig. 4). This is also true for a number of other estuaries in mediterannean climate regions - for example, Elkhorn Slough, California (Smith, 1973), Langebaan, South Africa (Christie, 1981), Peel-Harvey Estuary, W Australia (Hearn and Lukatelich, 1990), and Table 1. Representative data from five systems is presented in Fig. 5a. As hypersalinity occurs in response to evaporation, the longitudinal salinity structure reflects the length of time for which an average parcel of ocean water has been resident in the shallow evaporative basin. Observed residence times (Fig. 5c) are determined from a bulk (Lagrangian) salt balance:

$$T_{res} = (S - S_o)\, H_{av} / E_{av} S_{av} \qquad (2)$$

where S_o is the ocean salinity, assumed constant; H_{av}, E_{av} and S_{av} are average values for the basin during the period of residence. Inner Tomales Bay exhibits residence times of 40 to 100 days and in inner San Diego Bay water is resident for 10 to 40 days (Fig 5c).

If exchange rate and water depth were constant along the estuary, one would expect the residence time (and salinity) to increase lineary with distance from the mouth. However, the observed salinity distributions (Fig. 5a) indicate decreasing exchange towards the head of the basin. Analyzing salinity distributions $S(x)$ during late summer ($Q_f = 0$, $P = 0$), when salt content is constant, one can calculate $K_x(x) = -ExS \,/\, H\partial_x S$ from balancing advective and diffusive fluxes at each cross-section (see Eqn (1)) - these are plotted in Fig. 5b. Although diffusivities are large near the mouth, they are very small in the inner hypersaline part of these bays (of order 10 $m^2 s^{-1}$).

In the absence of density-driven vertical exchange, one expects dispersion to be dominated by the tidal to-and-fro motion. Following mixing length theory (Arons and Stommel, 1951; Officer, 1976, sections 2.5 and 5.5), tidal diffusivity should scale by $K_x(x) = kx^2$, as both velocity and length scales of tidal motion scale with x. Substituting into Eqn (1) with $\partial_t S = 0$, one can solve for $S(x)$:

$$S/S_o = (x \,/\, L)^{-E/kH} \tag{3}$$

Empirical values of $K_x(x)$ are obtained through fitting this solution to observed salinities. Towards the mouth, where $\partial_x S \to 0$, the error is large. Further into the bay, these curve-fitting estimates of K_x agree well with salt-balance estimates (Fig. 5b).

In comparison with the residence time given by Eqn (2) - how long a parcel of water has been in the basin - one can estimate a flushing time (how long it will take the observed hypersalinity to be diffused out of the system). This is expressed as:

$$T_{flush} = (S - S_o)\, x \,/\, K_x\, \partial_x S \tag{4}$$

This time scale roughly equals that for residence (Fig. 5c).

The largest errors in these empirical estimates of diffusivity and of time scales are due to variable $H(x)$ and due to large $K_x(x)$ near topographic features. Towards the head of the basin,

shallow depths increase the effectiveness of evaporation and observed salinities are larger than expected. Within a tidal excursion of the mouth, or other major morphological features, large K_x is expected as a result of tidal pumping and trapping processes (Fischer, et al, 1979, pp. 237-241; Geyer and Signell, 1992). The outer basin thus exhibits an oceanic character (Fig. 4). In estuaries with complex morphology (e.g., outer Mission Bay, Fig. 1), the assumptions of constant $H(x)$ and $W(x)$ are invalid and the hydrodynamic exchange is greater than that in simple, single-channel morphology. Short residence and oceanic conditions extend well into Mission Bay and hypersalinity develops only in the single channel of the inner basin (Figs. 2 and 5).

In summary, then, hypersalinity in temperate estuaries only occurs in those basins characterized by long, narrow, single-channel morphology (Table 1), where longitudinal tidal dispersion is weak (order 10 m^2s^{-1}). In warm hypersaline basins, observed longitudinal density gradients are typically too weak to be effective in buoyancy-driven exchange. While transient stratification due to inverse density gradients may be established (observed in San Diego Bay, Fig. 4; Mission Bay, Largier, et al, 1994; and Laguna Ojo de Liebre, Postma, 1965), very large longitudinal gradients are required before effective vertical exchange flows are established in these shallow basins. Linden and Simpson (1988) give $K_x \propto \partial_x \rho\, H^2$ for density-driven exchange, so that in a 10-m deep basin the density gradient must be 100 times larger than that required for the same diffusivity in a 100-m deep basin. In essence, buoyancy-driven exchange is negligible as compared with tidal exchange mechanisms in all three of the shallow basins discussed here.

The Occurrence of Hypersalinity and Its Ecological Importance

In spite of previous reports of hypersalinity in mediterranean-climate estuaries, the common and characteristic seasonal and longitudinal structures have received no attention. Based on observations from three Californian estuaries, these structures are explained by the seasonal cycles in freshwater gain/loss and by one-dimensional advection-diffusion exchange with the

ocean. Through a brief review of available data (Table 1), it appears that similar seasonally hypersaline estuaries are typical of mediterranean regions and that they comprise a major estuarine class.

The occurrence of hypersalinity requires a net evaporative loss $E > P + Q_f/Wx$ of water from an estuary that has a sufficiently long residence time. Long residence requires that $T_{res} \geq T_{evap}$, an evaporation time scale:

$$T_{evap} = (\sigma/S)\, H/(E - P - Q_f/Wx) \tag{3}$$

where σ is chosen such that $(S - S_o) > \sigma$ defines hypersalinity (see note 1). Whereas basins with large net evaporation and/or shallow water do not require long residence times to exhibit hypersalinity (e.g., Mission Bay), basins like Tomales Bay do require long residence times (Fig. 5).

The above flux and residence conditions are determined by three factors: (i) mediterranean *climate* with long dry summers; (ii) small *watershed* with short-tailed hydrograph; (iii) shallow *basin* with simple channel morphology. Climate, which determines $E(t)$, $P(t)$ and $Q_f(t)$, sets a potential latitude range from north of Tomales Bay to south of Bahia Magdalena (Fig. 1). The size, vegetation and geology of the watershed determines $Q_f(t)$. Northern San Francisco Bay (Conomos, et al, 1985), at similar latitude as Tomales Bay, does not exhibit hypersalinity as runoff from the large watershed persists throughout the dry summer. The tide and morphology of the estuarine basin determine the dispersion rate K_x and the residence time T_{res}. In Tomales Bay, simple morphology leads to small K_x and large T_{res} (Fig. 5), resulting in hypersalinity in spite of weak evaporation. Further, basin depth determines the effective evaporation E / H and the strength of the vertical mixing that suppresses buoyancy-driven exchange (and reduces K_x).

The occurrence of hypersalinity is subject to changes in the climate, watershed or basin, whether due to natural cycles/trends or due to the impact of human society. In particular, developments in the watershed may change both the volume and the shape of the hydrograph,

explain the observed concentrations of $DIP\,(x,t)$. Owing to the increased error in estimates of K_x as $\partial_x S$ approaches zero, the strength of the apparent sink in the outer bay is uncertain. Interannual variations in *DIP* concentration (compare 1988 and 1992) may be due to interannual variation in the hydrodynamic exchange or in the *DIP* source term. Occurring also in Langebaan (Christie, 1982), this phosphorus buildup appears to result from heterotrophic decomposition of particulate organic matter which releases *DIP*, *DIN* and carbon. Fixed nitrogen is consumed by the process of denitrification and one expects a ocean-to-atmosphere flux of carbon dioxide (Smith and McKenzie, 1987; Smith, et al, 1991). While these reactions may occur in all estuaries, the long residence times attained during the hypersaline phase of mediterranean estuaries allow the net signal to build up (Smith and Hollibaugh, 1989; Smith, et al, 1991; Kimmerer, et al, 1993).

The long residence times and limited longitudinal dispersion might also affect population dynamics or gene flow for a variety of species. Bacterioplankton in the inner portion of Tomales Bay are distributed conservatively with respect to salt during non-hypersaline periods, but they show net accumulation during periods of hypersalinity. Further, Kimmerer (1993) has reported discrete populations of closely related species of the copepod *Acartia* in Tomales Bay during the hypersaline season. Similarly, restricted dispersion of the meroplanktonic larvae spawned during hypersaline conditions might restrict gene flow, leading to genetic differentiation along an estuarine gradient or between populations in nearby estuaries.

These systems are very susceptible to pollution as even small loadings during the hypersaline phase may be recycled and accumulate rather than being flushed from the system. Interannual variation in residence time, due to interannual variation in the freshwater balance, may partially explain the interannual variation in metal loads observed in South San Francisco Bay benthic bivalve populations (Luoma, et al, 1985). Since socioeconomic development leads to both the extraction of water and the discharge of wastes, the concurrent increases in water

residence time and pollutant loading can lead to rapid and severe degradation of the water quality in these systems.

In conclusion, however, we note that seasonal hypersalinity is a natural state for some systems and that it does not denote degradation in itself. Such low-inflow mediterranean estuaries are, however, finely balanced and threatened by socio-economic development. Small changes in the freshwater budget of a basin with significant pollutant loading, or small increases in pollutant loading in a basin that exhibits long-residence hypersalinity, can lead to large accumulations and severe water quality problems. This threatens to destroy the health of these ecosystems. Left in a near-pristine state, as in Tomales Bay, this clearly defined hydrographic type has a clearly defined ecological and biogeochemical character. Although the hypersalinity probably does not dominate the hydrodynamics, nor the eco-dynamics, it is the defining symptom of long residence, limited freshwater inflow and reduced estuary-ocean exchange. It allows one to group together and study the common nature of the hydrodynamics and ecology of many individual basins found in mediterranean climate regions. Seasonal hypersalinity defines a major estuarine type - one that has been neglected.

ACKNOWLEDGEMENTS. This work was supported through the Land Margin Ecosystem Research (LMER) program of the National Science Foundation (Contracts #89-14833 and #89-14921), the California Department of Boating and Waterways (Interagency Agreements #91-100-080-19, #92-100-060-21 and #93-100-033-16), and the California State Water Resources Control Board (Interagency Agreement #1-188-190-0).

Note 1. In this work, we define "hypersaline" as "salinities significantly greater than that of the ambient" and "inverse" as "densities significantly greater than that of the ambient". By "salinities significantly greater" we conceive of a salinity S that exceeds the ambient salinity S_o by more than typical synoptic (ie., multi-day) fluctuations in the salinity of the ambient. The standard deviation of the ambient salinity over the period of hypersalinity, σ, serves as an appropriate index of the size of these fluctuations. Thus, $(S-S_o)>\sigma$ defines "hypersalinity". The value of σ is about 0.15 off Tomales Bay and 0.05 off Mission and San Diego Bays. Previously, hypersalinity has often been defined as salinities in excess of a fixed value (eg., 40 ppt, Day, 1981). While this may be physiologically meaningful, it is an arbitrary value otherwise and it provides no insight into the occurrence of hypersalinity, the salt balance or the associated hydrodynamics. For density, we prefer to think of "significantly greater" in terms of dynamics rather than statistics. A longitudinal density gradient of the order of 10^{-5} kg.m^{-4}, or greater, appears to be dynamically important in these shallow basins (depth of order 10 m).

References Cited

Arons, A. B. & Stommel, H. 1951 A mixing length theory of tidal flushing. *Trans. Am. Geophys. Union*, **32**, 419-421 (also *Woods Hole Oceanogr. Inst. Ref. No. 50-37*).

Bray, N. A. & Robles, J. M. 1991 Physical oceanography of the gulf of California. In: *The Gulf and Peninsular Province of the Californias* (J.P. Dauphin and B.R.T. Simoneit, eds.), AAPG Mem. 47, 511-533.

Chadwick, D. B., Largier, J. L. & Cheng, R. T. 1994 The role of thermal stratification in tidal exchange at the mouth of San Diego Bay. *Proceedings of 7th International Conference on the Physics of Estuaries and Coastal Seas* (submitted).

Christie, N. D. 1981 Primary production in Langebaan Lagoon. In: *Estuarine Ecology* (J.H. Day, ed.), Balkema, Rotterdam, 101-115.

Conomos, T. J., Smith, R. E. & Gartner, J. W. 1985 Environmental setting of San Francisco Bay. *Hydrobiologia*, **129**, 1-12.

Day, J. H. 1981 *Estuarine Ecology (with particular reference to southern Africa)*. Balkema, Rotterdam.

Denman, K. L. & Powell, T. M. 1984 Effects of physical processes on planktonic ecosystems in the coastal ocean. *Oceanogr. Mar. Biol. Ann. Rev.*, **22**, 125-168.

Fischer, H. B., List, E. J., Koh, R. C. Y., Imberger, J. & Brooks, N. H., *Mixing in Inland and Coastal Waters*, Academic Press, Boston, 483 pp (1979).

Geyer, W. R. & Signell, R. P. 1992 A reassessment of the role of tidal dispersion in estuaries and bays. *Estuaries*, **15(2)**, 97-108.

Gill, A. E., *Atmosphere-Ocean Dynamics*, Academic Press, Oxford, 500 pp. (1982).

Hearn, C. J. & Lukatelich, R. J. 1990 Dynamics of Peel-Harvey Estuary, Southwest Australia. In: *Residual Currents and Long-term Transport* (R.T. Cheng, ed.), Springer-Verlag, New York, 431-450.

Kimmerer, W. J. 1993 Distribution patterns of zooplankton in Tomales Bay, California. *Estuaries*, **16**(2), 264-272.

Kimmerer, W. J., Smith, S. V. and Hollibaugh, J. T. 1993 A simple heuristic model of nutrient cycling in an estuary. *Est. Coast. Shelf Sci.*, **37**. 145-159.

Lacombe, H. & Richez, C. 1982 The regime of the Straits of Gibraltar. In: *Hydrodynamics of Semi-enclosed Seas*, (J.C.J. Nihoul, ed.), Elsevier, Amsterdam, 13-73.

Langmuir, I. & Langmuir, D. B. 1927 *J. Phys. Chem.*, **31**, 1719.

Largier, J. L., Millikan, K. S. & Moore, T. 1994 Temperature and salinity structures in Mission Bay: A data report. *SIO Ref. Series*, (in press).

Linden, P. F. & Simpson, J. E. 1988 Modulated mixing and frontogenesis in shallow seas and estuaries. *Cont. Shelf Res.*, **8**, 1107-1127.

Luoma, S. N., Cain, D. & Johansson, C. 1985 *Hydrobiologia*, **129**, 109-120.

Nunes Vaz, R. A., Lennon, G. W. & Samarasinghe, J. R. de Silva 1989 The negative role of turbulence in estuarine mass transport. *Est. Coast. Shelf Sci.*, **28**, 361-377.

Nunes Vaz, R. A., Lennon, G. W. & Bowers, D. G. 1990 Physical behaviour of a large, negative or inverse estuary. *Cont. Shelf Res.*, **10**, 3, 277-304.

Officer, C. B. 1976 *Physical Oceanography of Estuaries (and Associated Coastal Waters)*. John Wiley, New York, 465 pp.

Pages, J. & Debenay, J.-P. 1987 Evolution saisonniere de la salinite de la Cassamance. *Rev. Hydrobiol. trop.* **20** (3-4), 191-202 and 203-217.

Phillips, O. M. 1966 On turbulent convection currents and the circulation of the Red Sea. *Deep-Sea Res.*, **13**, 1149-1160.

Postma, H. 1965 Water circulation and suspended matter in Baja California lagoons. *Neth. J. Sea Res.*, 2(4), 566-604.

Pritchard, D. W. 1967 Observations of circulation in coastal plain estuaries. In: *Estuaries*

(G.H.Lauff, ed.), AAAS Publ. #83, Washington, 37-44.

Smith, N. P. 1988 The Laguna Madre of Texas: hydrography of a hypersaline lagoon. In: *Hydrodynamics of Estuaries, Volume II, Estuarine Case Studies* (B.Kjerve, ed.), CRC Press, Boca Raton.

Smith, R. E. 1973 The hydrography of Elkhorn Slough: a shallow California coastal embayment. *Moss Landing Marine Laboratories, Tech. Publ. 73-2.*

Smith, S. V. & Hollibaugh, J. T. 1989 Carbon-controlled nitrogen cycling in a marine 'macrocosm': an ecosystem-scale model for managing cultural eutrophication. *Mar. Ecol. Prog. Ser.* **52**, 103-109.

Smith, S. V. & Mackenzie, F. T. 1987 The ocean as a net heterotrophic system: implications from the carbon biogeochemical cycle. *Global Biogeochem. Cycles*, **1**, 187-198.

Smith, S. V., Hollibaugh, J. T., Dollar, S. J. & Vink, S. 1991 Tomales Bay metabolism: C-N-P stoichiometry and ecosystem heterotrophy at the land-sea interface. *Estuarine Coastal Shelf Sci.*, **33**, 223-257.

Wolanski, E. 1986 An evaporation-driven salinity maximum zone in Australian tropical estuaries. *Est. Coast. Shelf Sci.*, 22, 415-424.

Figure Captions

Figure 1. (a) Estuaries along the west coast of North America in which summer hypersalinity has been reported (see also Table 1); (b) Tomales Bay, indicating station positions and the region of summer hypersalinity (shaded); (c) Mission Bay, indicating region of summer hypersalinity (shaded) and positions of stations in that region. (d) San Diego Bay, indicating station positions and region of summer hypersalinity (shaded)

Figure 2. The seasonal variation in temperature, salinity, and density in Mission Bay. At station 21 (farthest from ocean, Figure 1c), surface values (open circles), bottom values (crosses), and vertical average values (bold line) are plotted. For comparison, vertical average values are also plotted for station 9, at the landward extent of the well-flushed outer estuary (dashed line), and for a station at the end of the pier at Scripps Institution of Oceanography, several kilometers north of the mouth (solid line). The period during which station 21 is warmer, saltier or denser than the ocean is indicated by shading. Stratification is not observed in the hypersaline inner estuary. The date marks indicate the dates at which hypersaline and inverse conditions start and end.

Figure 3. The seasonal variation in the longitudinal structure of temperature T, salinity S, density ρ, dissolved inorganic phosphorus DIP and dissolved inorganic nitrogen DIN and in the freshwater budget terms for Tomales Bay. The value at each grid point (indicated by a dot) is the average of data collected during several hydrographic surveys over a 10-day period. In the top five panels, diagonal hatching highlights summer extrema ($T > 17°C$; $S > 34$; DIP > 2 mmol.m^{-3}; DIN < 1 mmol.m^{-3}) and horizontal hatching highlights winter extrema ($T < 14°C$; $S < 31$; $\rho < 1023.5$ kg.m^{-3}; DIN > 10 mmol.m^{-3}). In the density panel, dark shading indicates local maxima. The bold isolines in density and DIN are levels of 1025.0 kg.m^{-3} and 4

mmol.m^{-3}, respectively. Contour intervals are 1°C, 1, 0.5 kg.m^{-3}, 0.5 mmol.m^{-3} and 3 mmol.m^{-3} for T, S, ρ, DIP and DIN, respectively. In the lowest panel, stream inflow Q_f (dotted line), precipitation P (dot-dash line), evaporation E (dashed line) and net freshwater inflow (bold line) are given as volume flow rates divided by surface area - summer periods of net loss are indicated by diagonal hatching.

Figure 4. An example of typical (a) temperature, (b) salinity and (c) density structures observed in San Diego Bay during summer hypersaline conditions. These data are for a spring flood tide, between 09:25 and 11:54 on 10 August 1993. Data points are indicated by dots (see station positions in Fig. 1d). The mouth is at a distance of 26 km from the head of the estuary. Contour intervals are 1° C, 0.2 ppt and 0.2 kg.m^{-3}, respectively.

Figure 5. Longitudinal variation in (a) observed salinity (normalized by salinity at mouth), (b) calculated values of longitudinal diffusivity K and (c) calculated values of a residence time scale T_{res} in selected estuaries. Observations are from late summer, when salinities are steady ($d_t S$ = 0): (i) data for Tomales Bay are a 6-year average of the September values shown in Figures 3 and 6; (ii) Mission Bay data are averaged over a single tidal cycle in August 1992; (iii) San Diego Bay data are an average of 3 surveys in August 1993; (iv) Elkhorn Slough data are an average over the month of August 1971, as reported by Smith (1973); (v) Langebaan data are averaged over 5 monthly surveys in the 1975-76 summer (Christie, 1981).

(a) Lines are a best fit of $(S/S_o) = a.(x/L)^{-b}$, which is Eq. (3) with an arbitrary factor to account for the difference between mouth salinities and the salinity of the ambient. For Mission Bay, only the back-estuary exhibits hypersalinity and the water at station 9 is taken as ambient, so that L = 4.2 km (Figure 1c).

(b) Symbols indicate diffusivities $K_x = -E\ x\ S/H\partial_x S$ and lines indicate diffusivities obtained from the best-fit line in the top panel (see Eq. (3)). Distance is not normalized, but rather plotted

as distance from the head, where $K_x = 0$ for all systems. (c) Symbols indicate residence time T_{res} from Eq. (2) and lines indicate flushing time from Eq. (4), where K_x values are from the lines in the second panel. Distance is plotted relative to the mouth, where residence time should go to zero for all systems. In estimates of both diffusivity and residence time, the error near the mouth grows as $d_x S$ tends to zero.

Figure 6. Longitudinal variation in (a) observed salinity, (b) observed *DIP* concentration and (c) estimated *DIP* production for 6 summers (1987-1992) at Tomales Bay (cf. Figure 3). Data are from September, when salinities are quasi-steady. In the top panel, observed salinities are indicated by symbols and lines indicate the best fit of Eq. 3 for 1988 and 1992, the driest and wettest summers, respectively (Fig. 2). As dispersion is dominated by tidal motions, the same diffusivity is expected for the hypersaline period in all years. Using this diffusivity in a one-dimensional *DIP* balance, one can determine what non-conservative *DIP* term is required to explain the observed *DIP* concentrations (symbols in middle panel). The calculated *DIP* production is plotted in the lower panel - indicating a coherent *DIP* source in the slow-flushing inner bay where the model and data agree well (Fig. 5). The *DIP* sink predicted in the outer bay is not well defined as the error in this model increases towards the mouth as $\partial_x S$ approaches zero. The lines in the middle panel are estimates of the potential accumulation of *DIP* obtained by multiplying the estimated production (lower panel) by residence time $T_{res}(x)$ (from Fig. 5).

Fig. 1

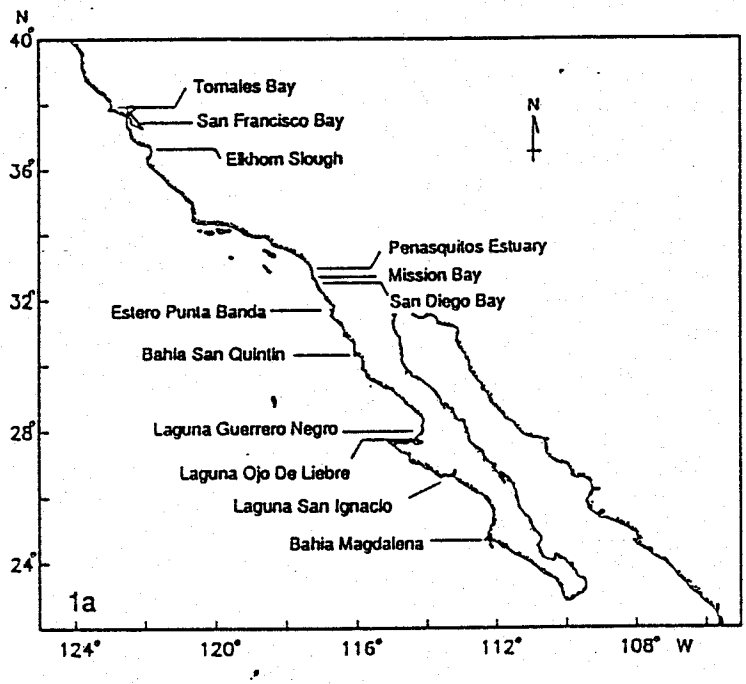
N
40°
36°
32°
28°
24°
Tomales Bay
San Francisco Bay
Elkhorn Slough
Penasquitos Estuary
Mission Bay
San Diego Bay
Estero Punta Banda
Bahia San Quintin
Laguna Guerrero Negro
Laguna Ojo De Liebre
Laguna San Ignacio
Bahia Magdalena
1a
124°
120°
116°
112°
108° W

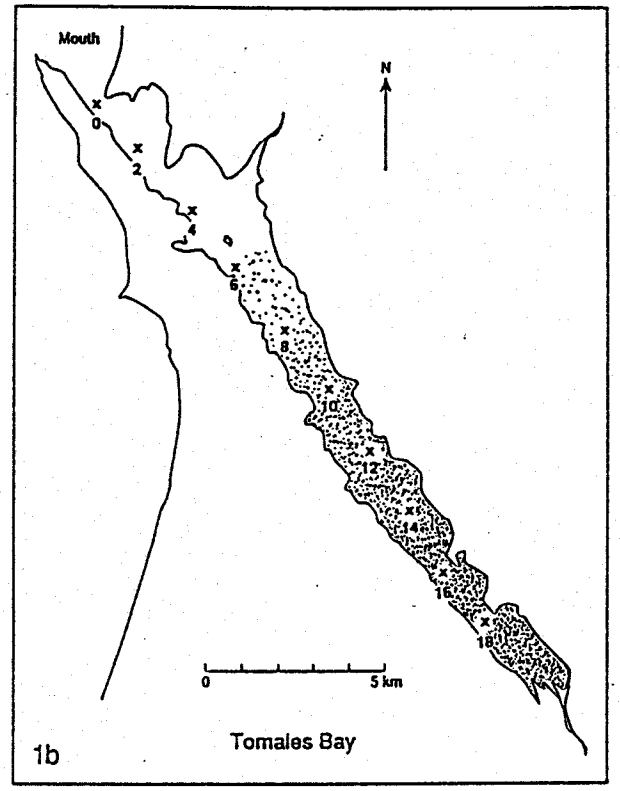
Mouth
N
0
2
4
6
8
10
12
14
16
18
0
5 km
1b
Tomales Bay

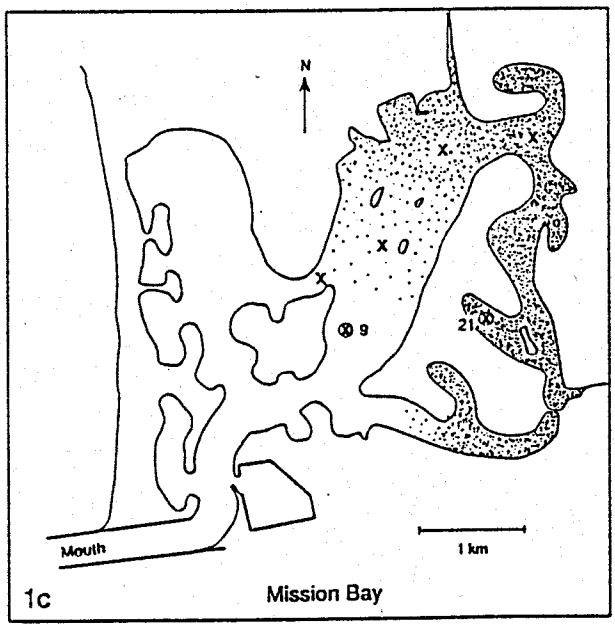
N
9
21
Mouth
1 km
1c
Mission Bay

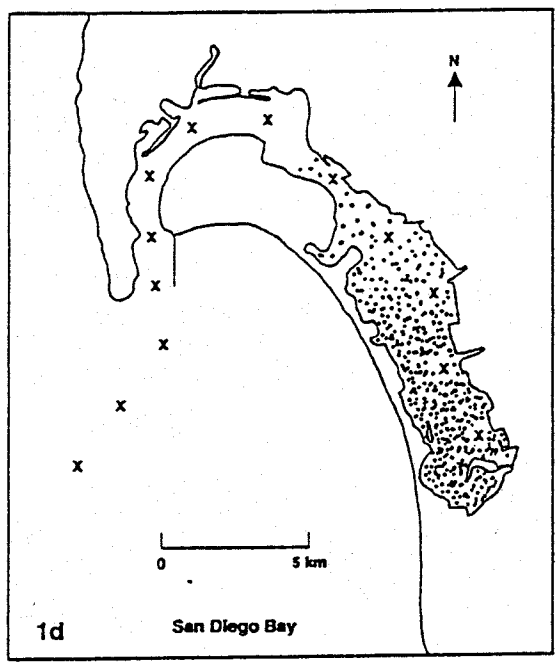
N
0
5 km
1d
San Diego Bay

Fig. 2

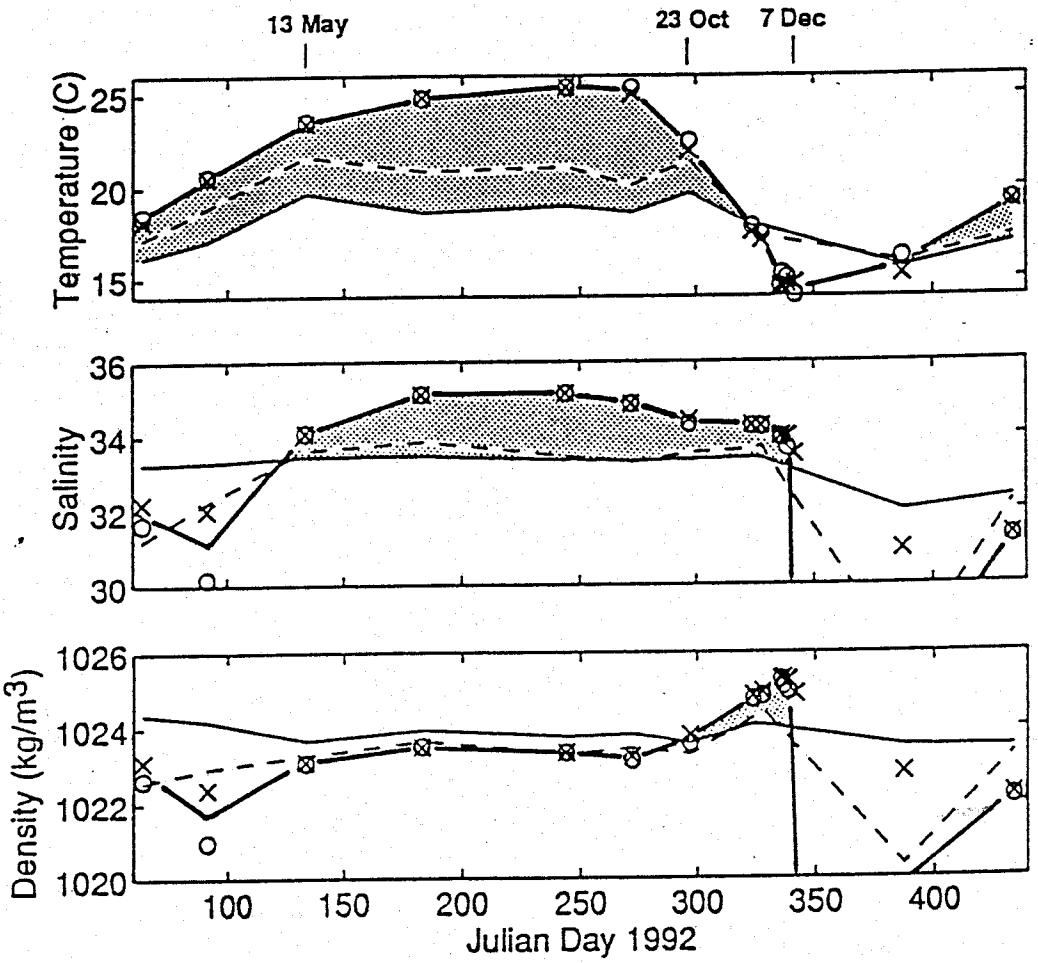
13 May
23 Oct
7 Dec
Temperature (C)
25
20
15
Salinity
36
34
32
30
Density (kg/m3)
1026
1024
1022
1020
100
150
200
250
300
350
400
Julian Day 1992

Fig. 3.

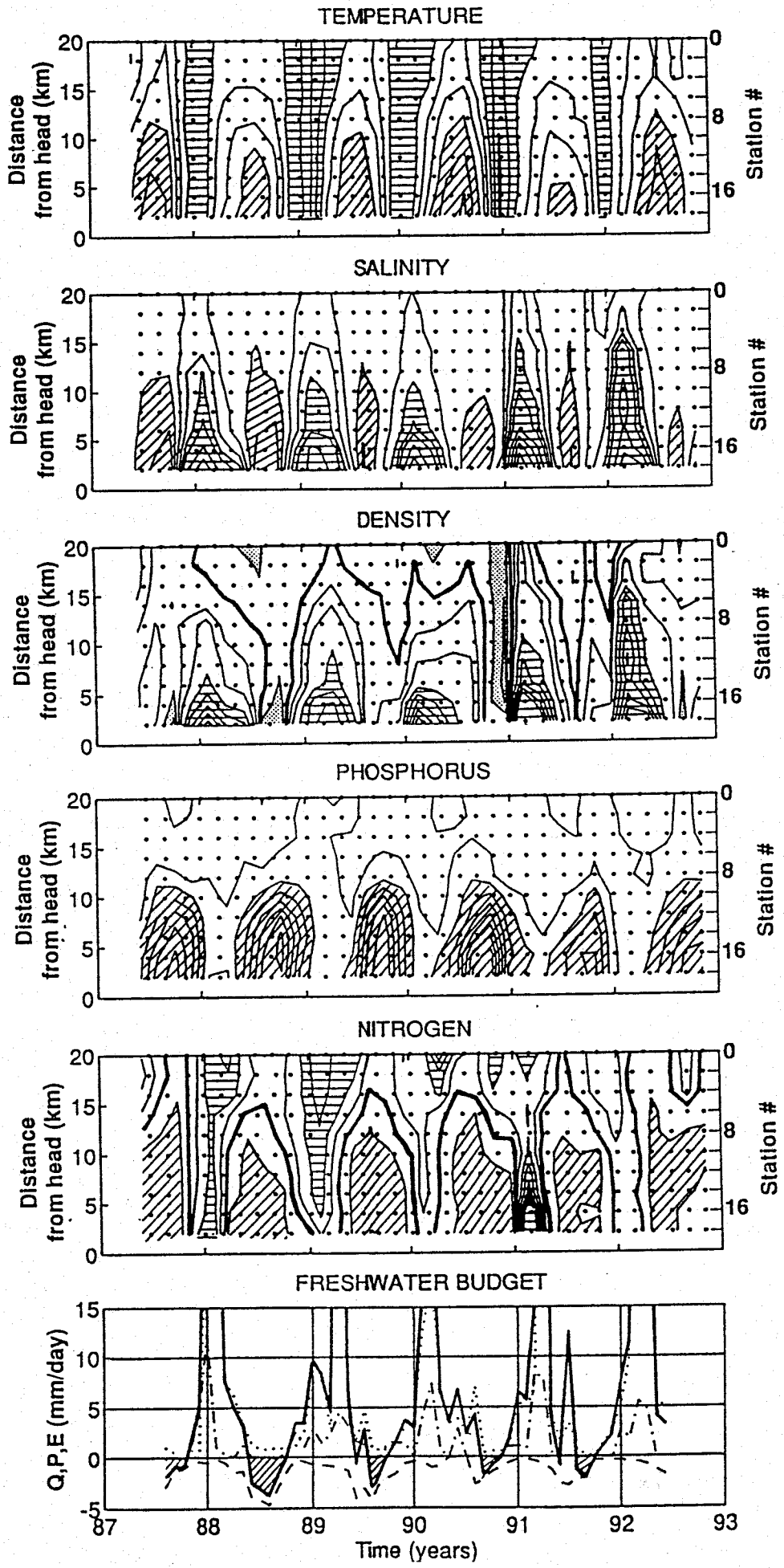
TEMPERATURE
SALINITY
DENSITY
PHOSPHORUS
NITROGEN
FRESHWATER BUDGET
Distance from head (km)
Station #
0
5
10
15
20
8
16
Q,P,E (mm/day)
-5
87
88
89
90
91
92
93
Time (years)

Fig. 4.

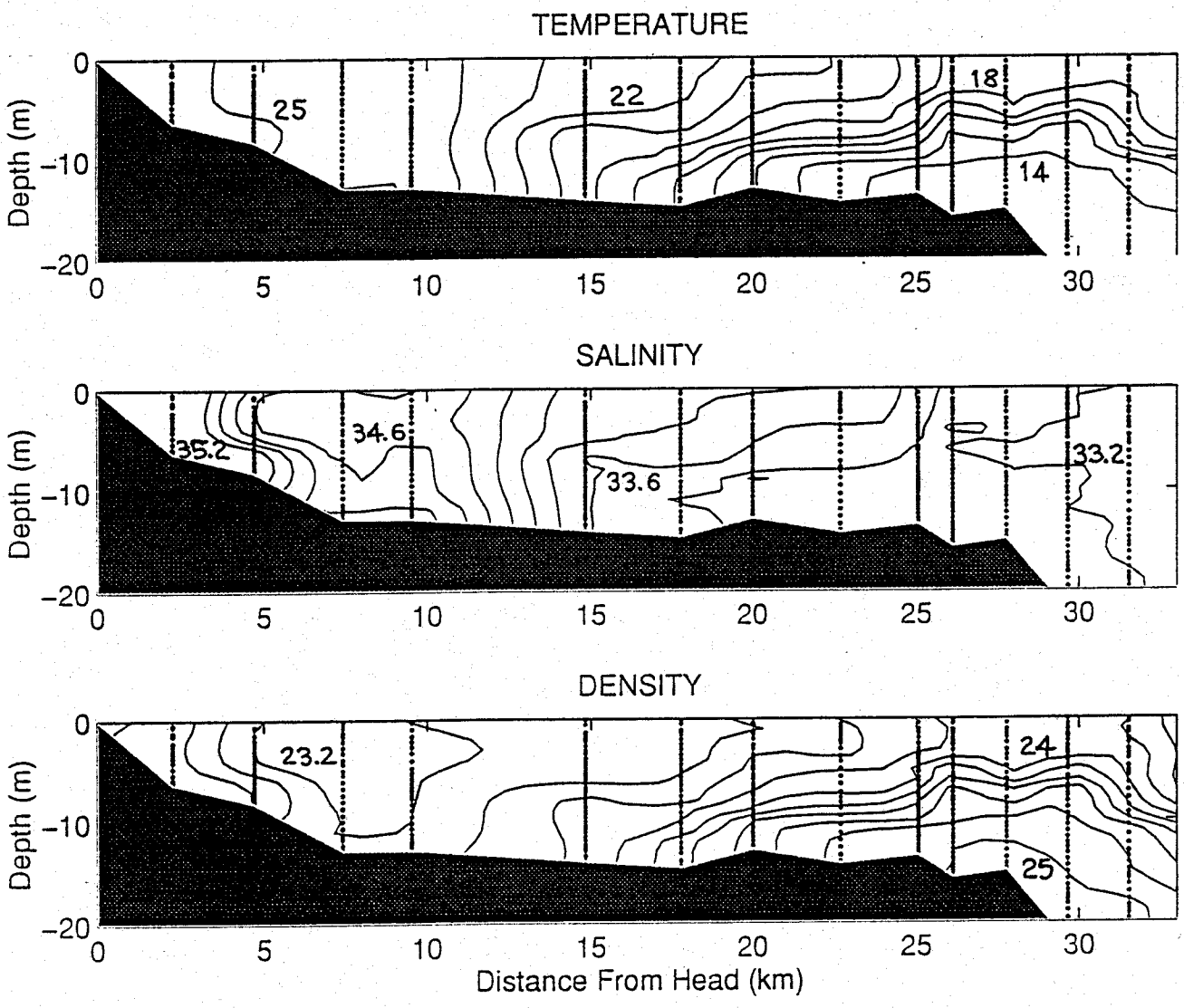
TEMPERATURE
Depth (m)
0
−10
−20
25
22
18
14
0
5
10
15
20
25
30
SALINITY
Depth (m)
0
−10
−20
35.2
34.6
33.6
33.2
0
5
10
15
20
25
30
DENSITY
Depth (m)
0
−10
−20
23.2
24
25
0
5
10
15
20
25
30
Distance From Head (km)

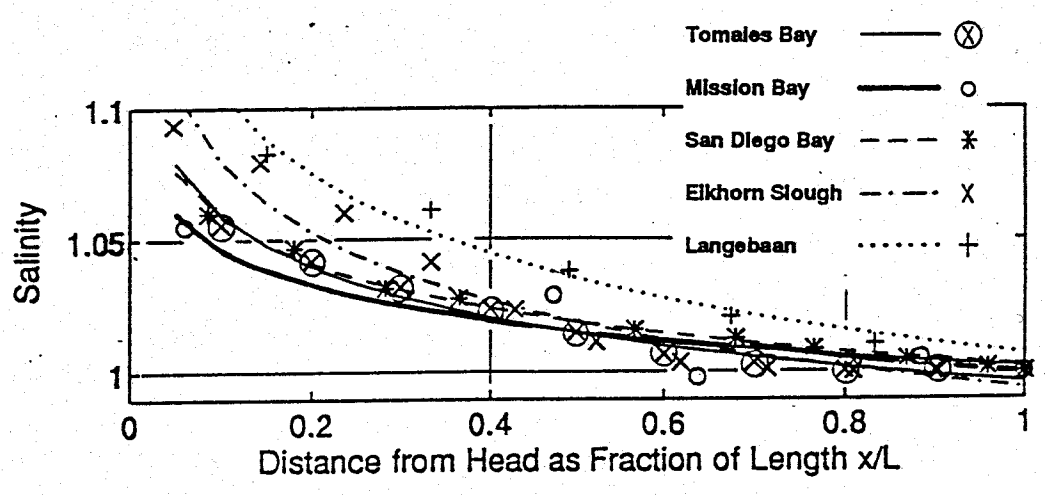
Tomales Bay
Mission Bay
San Diego Bay
Elkhorn Slough
Langebaan
Salinity
1.1
1.05
1
0
0.2
0.4
0.6
0.8
1
Distance from Head as Fraction of Length x/L

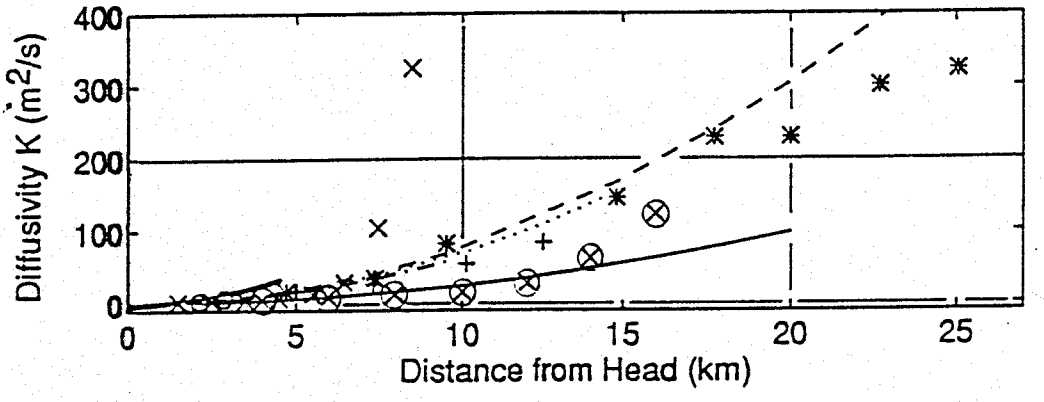
Diffusivity K (m2/s)
400
300
200
100
0
0
5
10
15
20
25
Distance from Head (km)

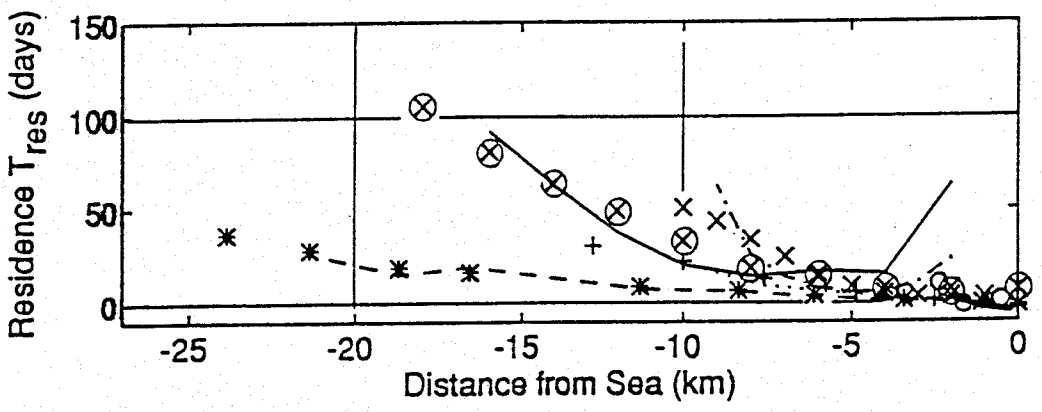
Residence Tres (days)
150
100
50
0
-25
-20
-15
-10
-5
0
Distance from Sea (km)

Fig. 6.

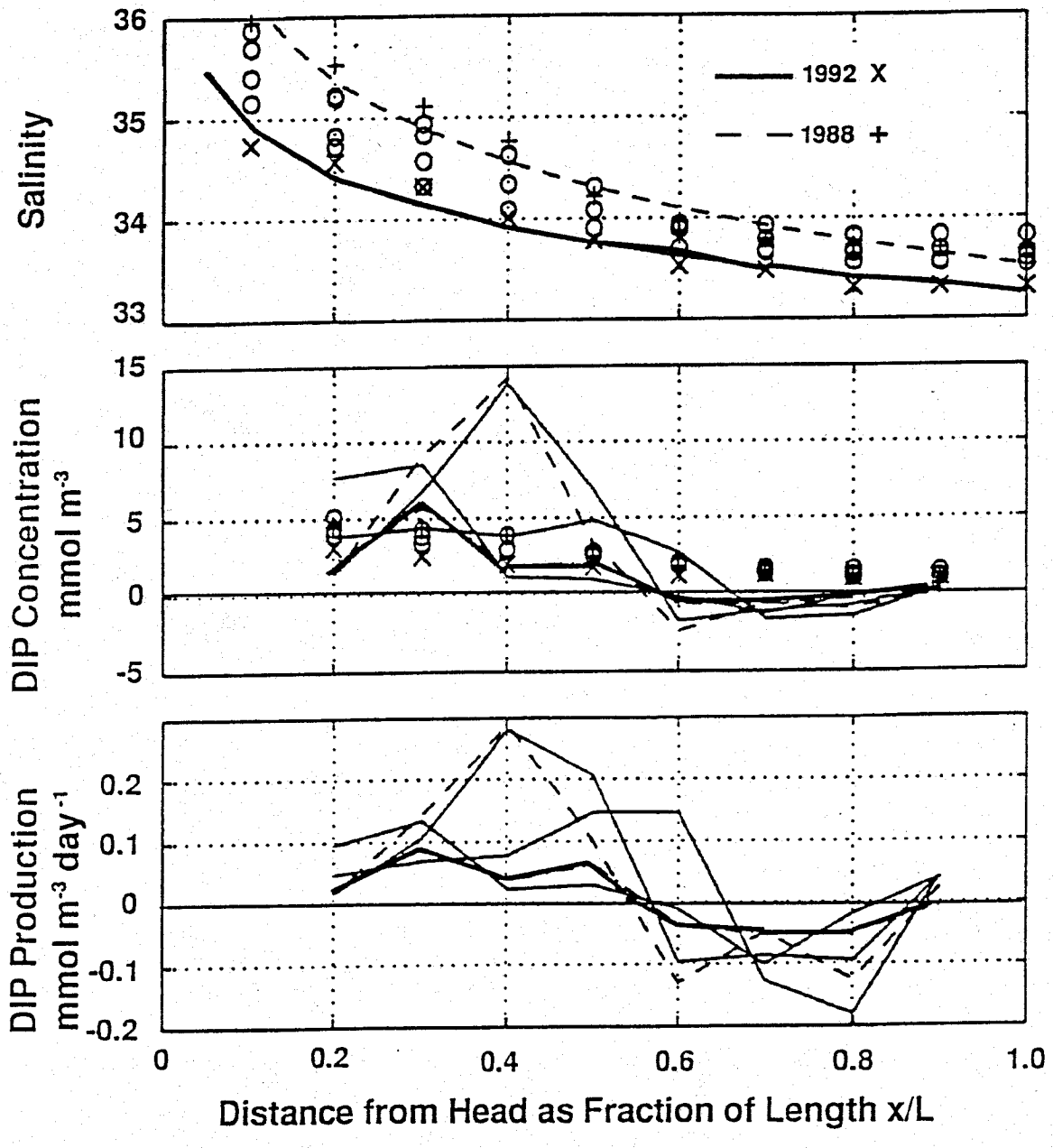
Salinity
36
35
34
33
1992 X
1988 +
DIP Concentration
mmol m-3
15
10
5
0
-5
DIP Production
mmol m-3 day-1
0.2
0.1
0
-0.1
-0.2
0
0.2
0.4
0.6
0.8
1.0
Distance from Head as Fraction of Length x/L